Supporting Information

Injectable Vitreous Substitute Sustained Release Metformin for Enhanced Uveal Melanoma Immunotherapy

Muyue Yang‡, Jipeng Li‡, Zeyang Liu‡, Haiyang Zhang, Jin Liu, Yan Liu, Ai Zhuang, Huifang Zhou, Ping Gu*, Xianqun Fan**

Department of Ophthalmology, Shanghai Ninth People's Hospital, Shanghai Jiaotong University School of Medicine, Shanghai 200011, China. Shanghai Key Laboratory of Orbital Diseases and Ocular Oncology, Shanghai 200011, China.

Correspondence to:

Huifang Zhou[a], Ping Gu[b], Xianqun Fan[c]

[a]E-mail: fangzzfang@163.com

[b]E-mail: guping2009@126.com

[c]E-mail: fanxq@sjtu.edu.cn

‡These authors equally contributed to this work.

1. Supplementary figures

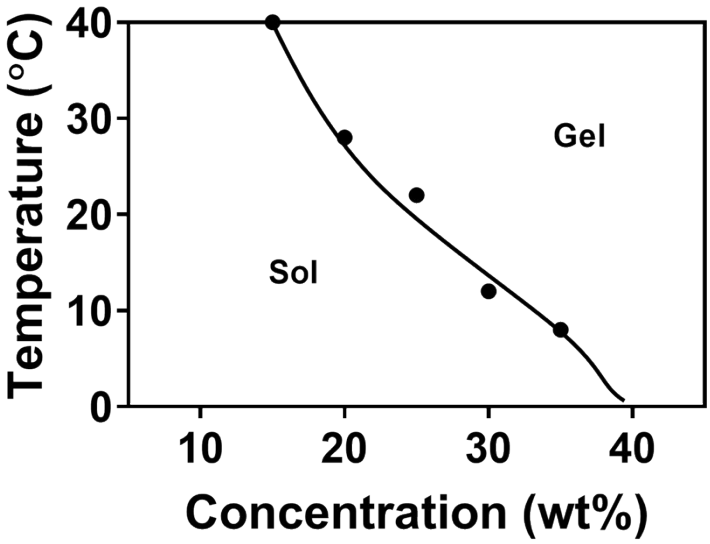

Figure S1. The phase diagram of IVS. IVS (20 wt%) underwent a thermo-sensitive sol-gel transition at approximately 27 ℃.

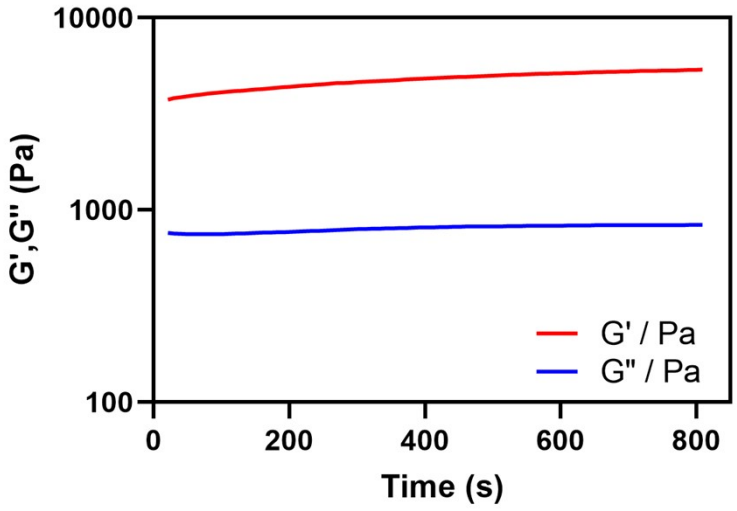

Figure S2. Rheological test of IVS in a time sweep mode. Variation of dynamic storage moduli G′ and loss moduli G″ of IVS in a time sweep mode at 37 °C. G′ was higher than G″, suggesting a stable gel state of IVS at 37 °C.

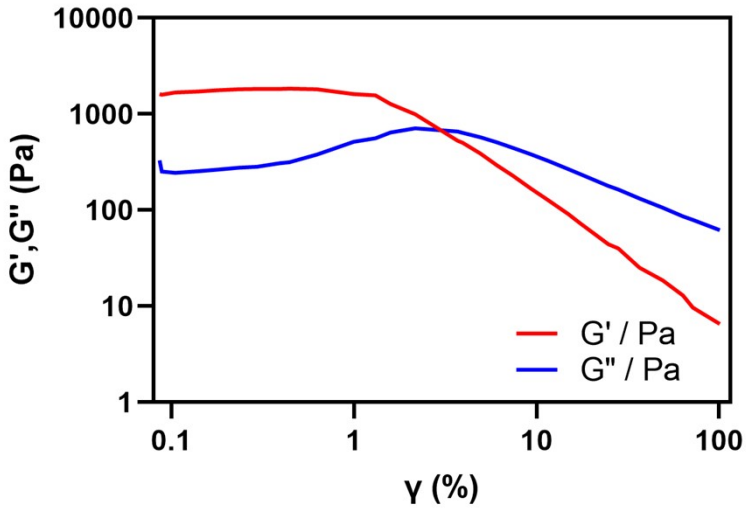

Figure S3. Rheological test of IVS in an amplitude sweep mode. Variation of dynamic storage moduli G′ and loss moduli G″ of IVS in an amplitude sweep mode at 37 °C.

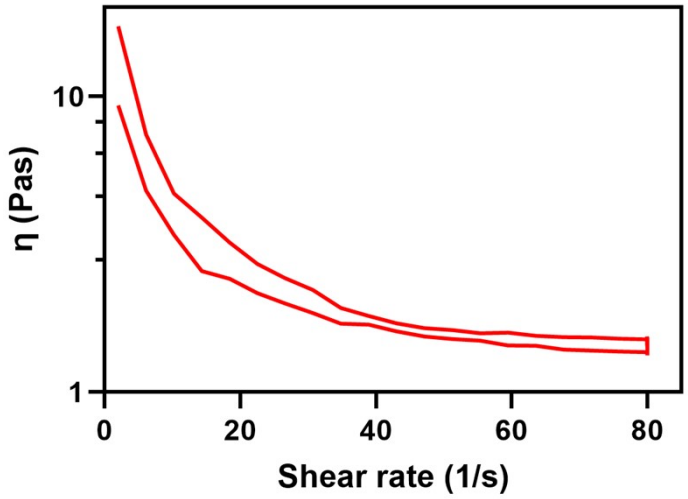

Figure S4. The viscosity curve of IVS. The viscosity of IVS rapidly decreased when the shear rate increased from 2 to 80 s^{-1}, while gradually recovered when shear rate decreased, demonstrating the recovery ability of IVS.

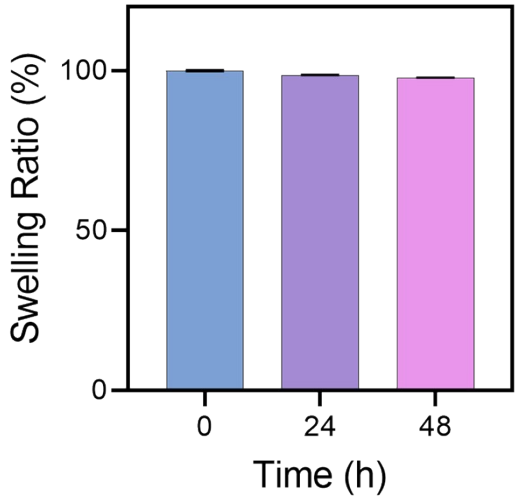

Figure S5. The swelling ratio of IVS. No significant swelling of IVS was observed up to 48 h, thus avoiding high intraocular pressure due to unexpected swelling of IVS after injection into eyeballs.

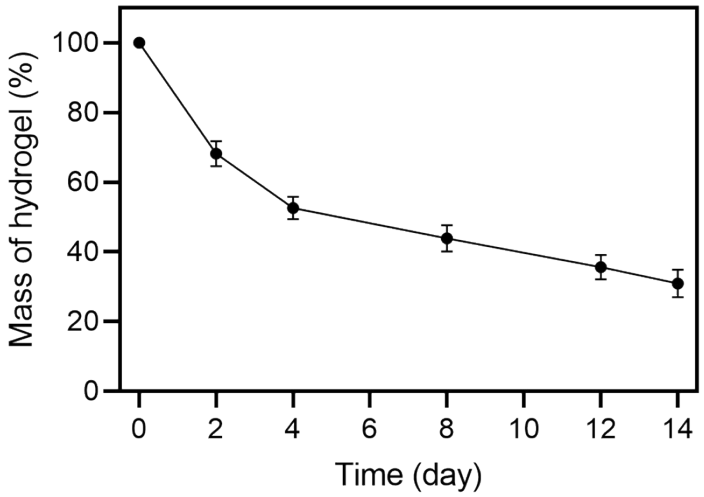

Figure S6. The *in vitro* degradation behavior of IVS (20 wt%) in PBS containing 20% FBS (n=3).

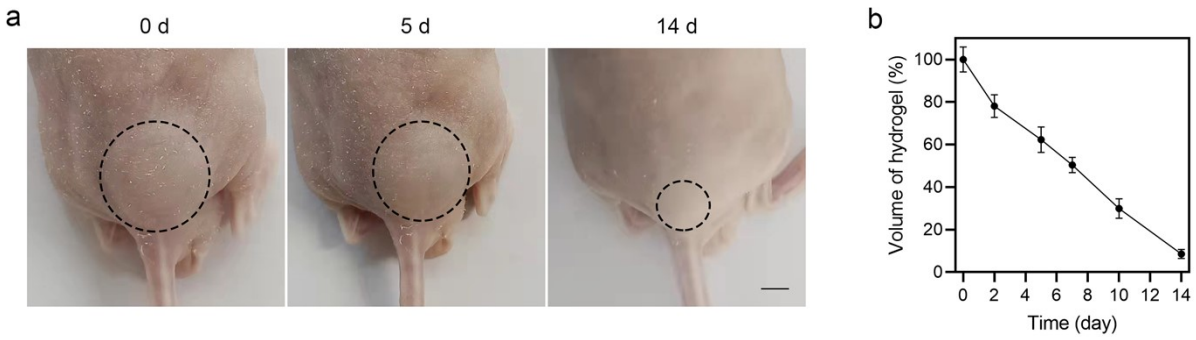

Figure S7. *In vivo* degradation behavior of IVS. a) The outline of IVS on 0, 5, and 14 d was indicated by the black dotted lines. IVS largely degraded by 14 days, avoiding secondary surgeries. Scale bar: 50 cm. b) Quantitative analysis of the volume of hydrogel (n = 3).

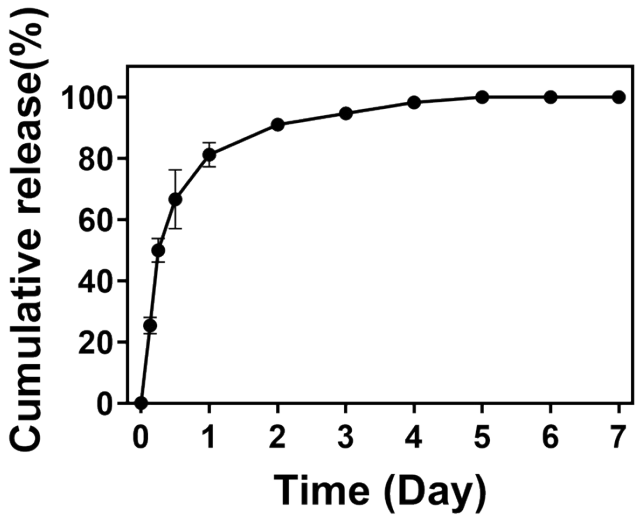

Figure S8. Cumulative release of metformin from IVS-Met. IVS-Met prolonged the release of metformin up to 5 days *in vitro*.

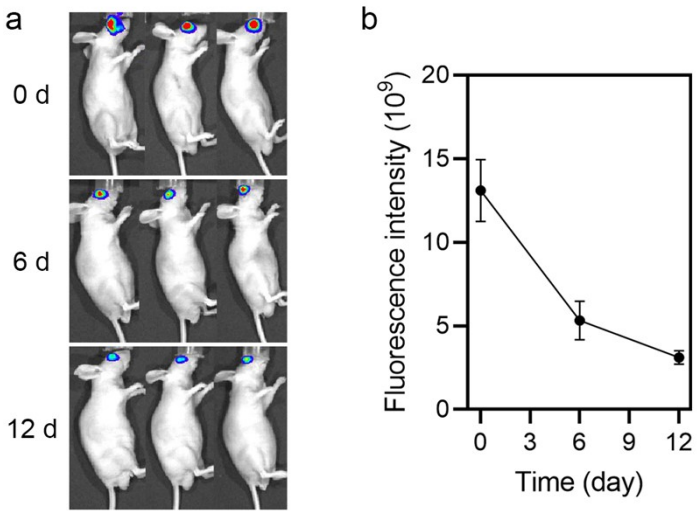

Figure S9. The *in vivo* release kinetics of metformin. a) IVS-Met was labeled by Cy5.5 and injected into eyeballs, and then monitored by the IVIS Lumina system at different time points. b) Quantitative analysis of the fluorescence intensity (n = 3).

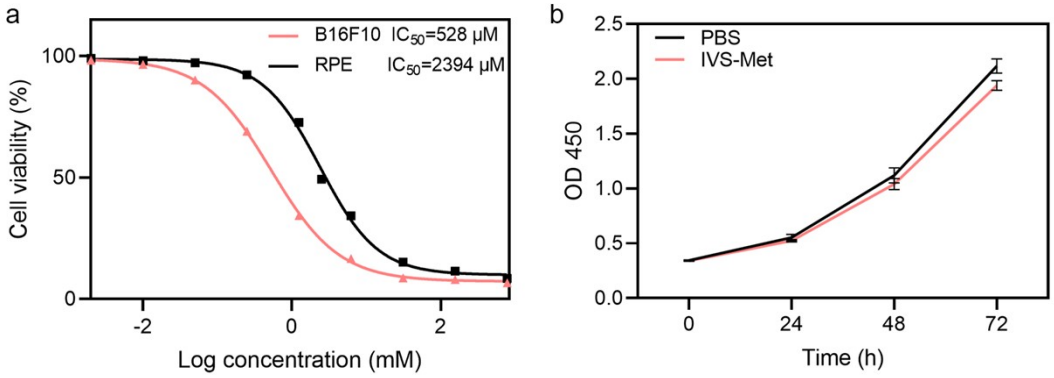

Figure S10. a) Cell viability of tumor cell (B16F10 cell) and normal cells (RPE cell) after treatment with various concentrations of metformin. The IC50 values are listed after the cell names. b) Cell viability of RPE cell treated with 1 mM of metformin tested by CCK-8 assay. 1 mM of metformin did not show obvious inhibitory effect on the proliferation of normal cells. The absorbance at 450 nm was recorded and is presented as the mean ± SD (n = 3).

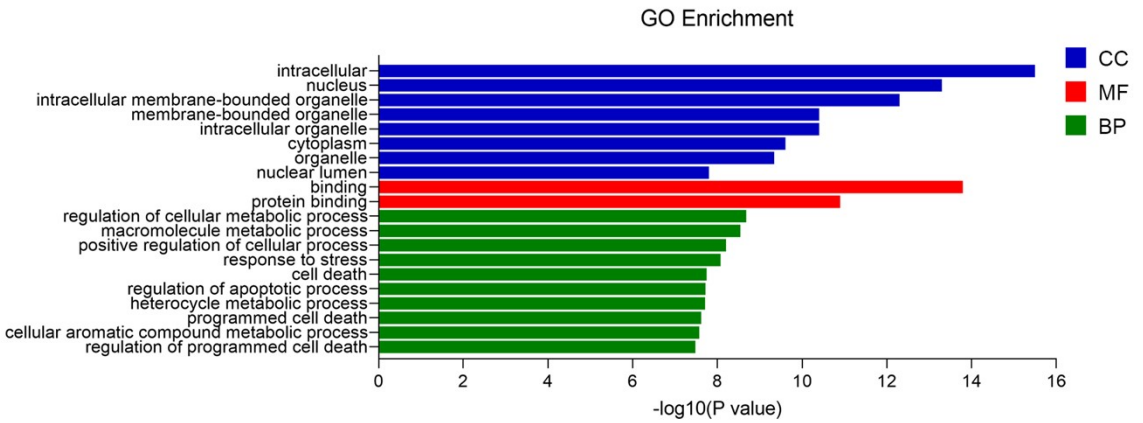

Figure S11. The GO enrichment analysis of differentially expressed genes. The GO analysis classified differentially expressed genes to cellular components (CC), biological process (BP) and molecular function (MF) according to the molecular function of genes. The result indicated that IVS-Met mainly affected the genes participating in the regulation of apoptotic process and cellular metabolic process.

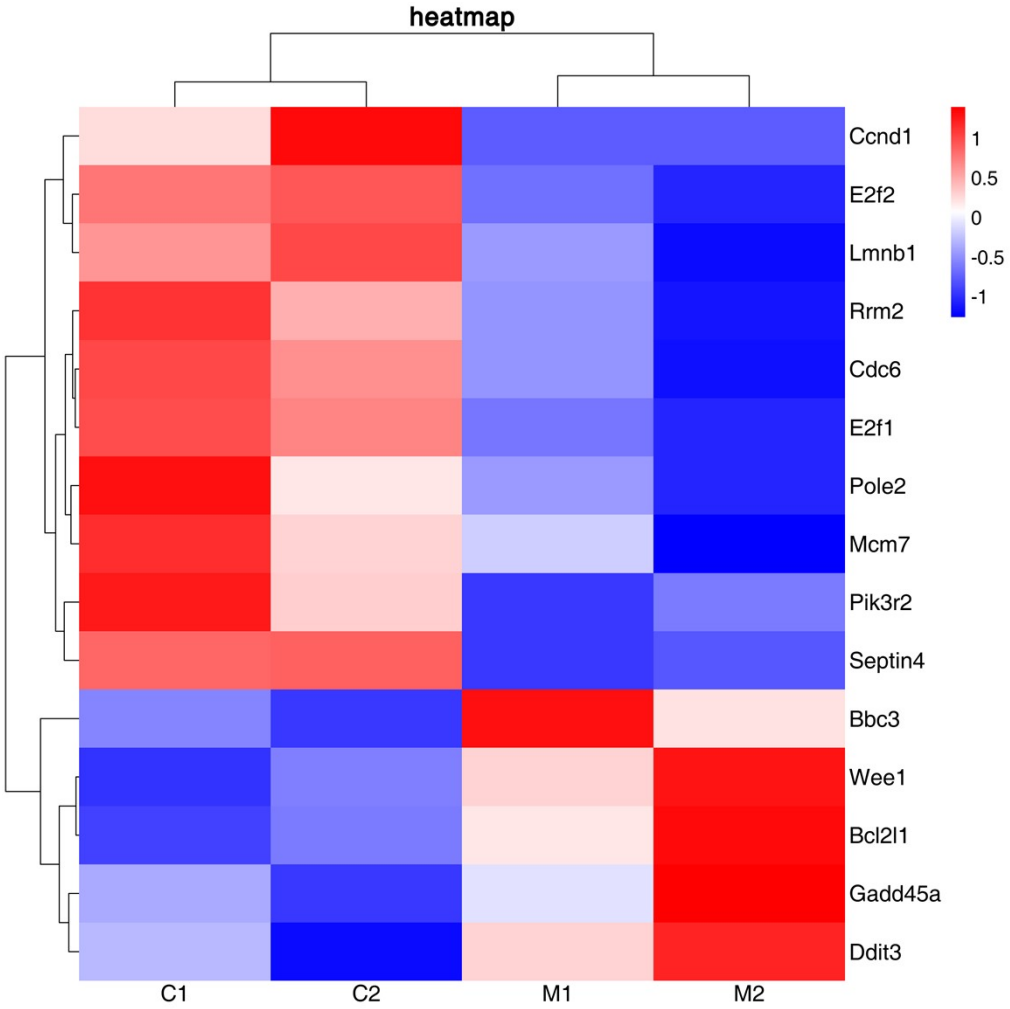

Figure S12. The heatmap of differentially expressed genes associated with cell cycle and apoptosis. Differentially expressed genes between B16F10 (C1-C2) and B16F10 treated with IVS-Met (M1-M2). Red corresponds to up-regulation; blue to down-expression. The result suggested that IVS-Met induced the cell cycle arrest and enhanced apoptotic process.

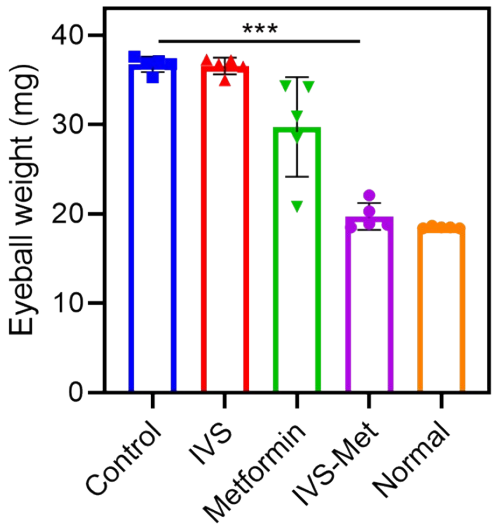

Figure S13. The weight of eyeballs in control, IVS, metformin and IVS-Met group. The eyeballs in each group were harvested from the orthotopic UM-bearing mice on 15 d and weighed (n = 5). Data are presented as the mean ± SD. Statistical analysis was performed using Student's *t*-test (*** $P < 0.001$).

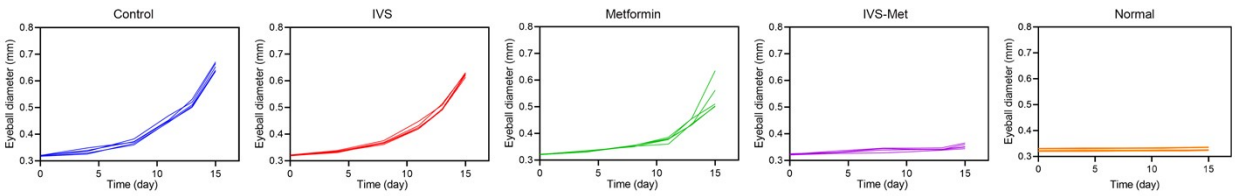

Figure S14. Growth curve of tumor in each group. The growth of tumor was recorded by eye diameter in each mouse from 0 d to 15 d (n = 5).

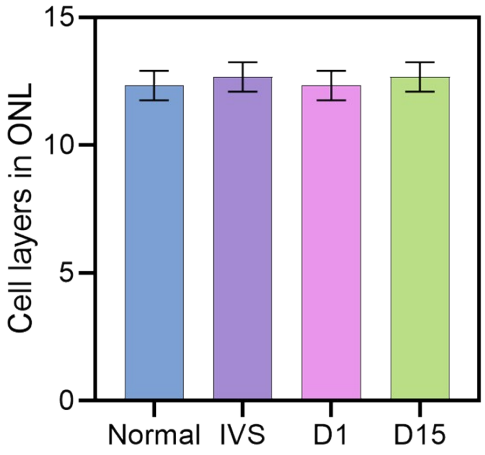

Figure S15. Biocompatibility of the IVS-Met on retinal cells. Quantitative analysis of the number of cell layers in the outer nuclear layer (ONL) in each group (n = 3). No significant difference was observed after IVS-Met treatment, demonstrating high biocompatibility of the IVS-Met on retinal cells.

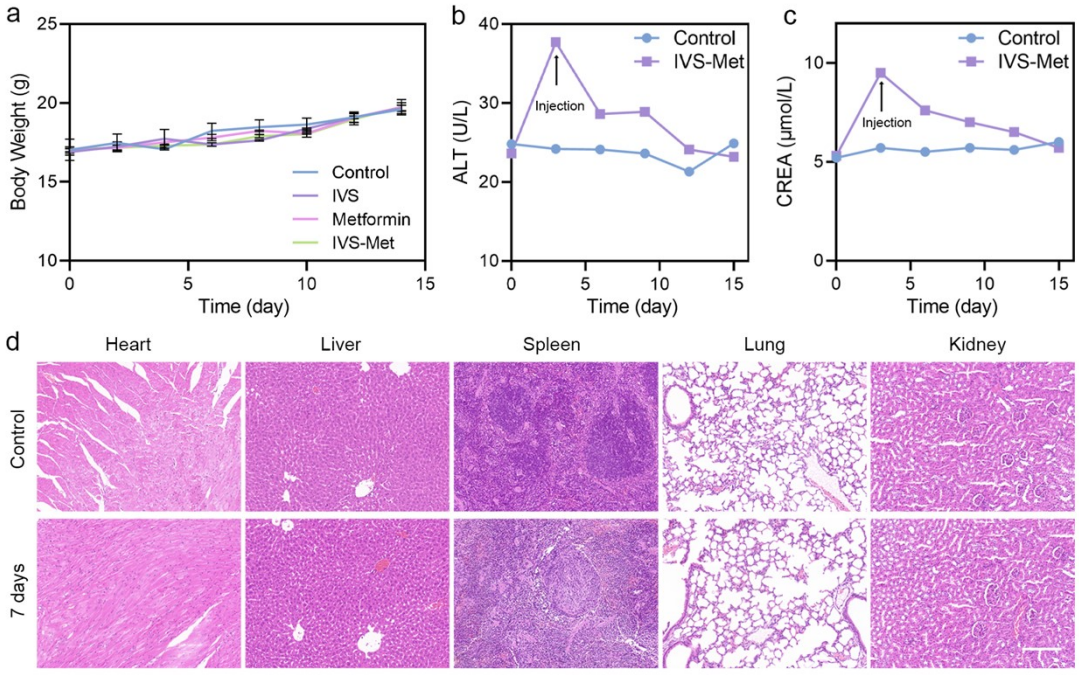

Figure S16. Biocompatibility of IVS-Met. a) The body weight of mice in each group. b) The serum levels of the hepatic function marker alanine aminotransferase (ALT). When IVS-Met was injected, the concentration of ALT increased, however, it returned to normal within

3 days. c) The serum levels of the renal function marker creatinine (CREA). After IVS-Met was injected, the concentration of CREA increased, but returned to normal in 3 days. d) The HE images of major organs (heart, liver, spleen, lung, and kidney) from control and IVS-Met-treated mice. No signs of inflammation, cell necrosis, or apoptosis were observed in the tissues of mice treated with IVS-Met. Scale bar: 100 μm.

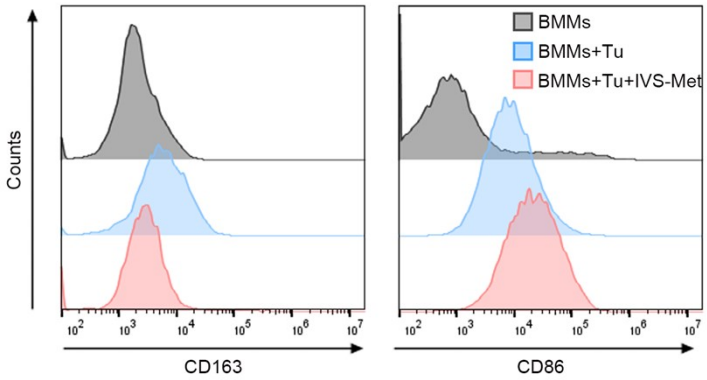

Figure S17. TAM polarization evaluated by histograms of the cell surface expression of CD163 and CD86 in each group. After co-incubated with tumor cells (BMMs+Tu), the expression of M2-associated CD163 in BMMs increased. After treated with tumor cells and IVS-Met (BMMs+Tu+IVS-Met), the expression of CD163 decreased, while the expression of M1-associated CD86 increased, revealing that IVS-Met reduced the proportion of M2 TAMs and induced M1 TAMs in TME.

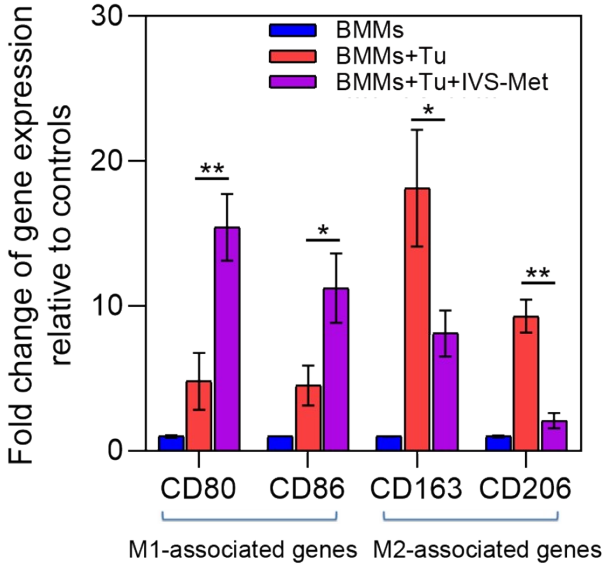

Figure S18. RT-qPCR analysis of the levels of expression of M1-associated (CD80 and CD86) or M2-associated (CD163 and CD206) genes. Data are presented as the mean ± SD (n = 3). Statistical analysis was performed using Student's *t*-test (* $P < 0.05$, ** $P < 0.01$).

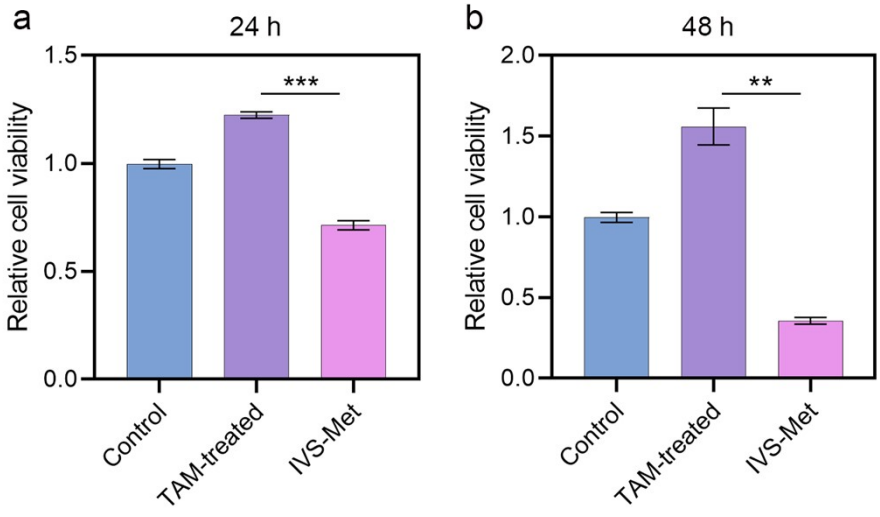

Figure S19. The proliferative ability of tumor cells after various treatment. The cell viability of B16F10 cells in control (without treatment), TAM-treated (co-incubated with TAMs), and IVS-Met (treated with TAMs and IVS-Met) group at 24 h (a) and 48 h (b). The statistical significance was measured by Student's *t*-test (** $P < 0.01$, *** $P < 0.001$). Tumor

cells exhibited enhanced proliferative ability when co-incubated with TAMs. However, the viability of tumor cells was significantly inhibited after treatment with IVS-Met.

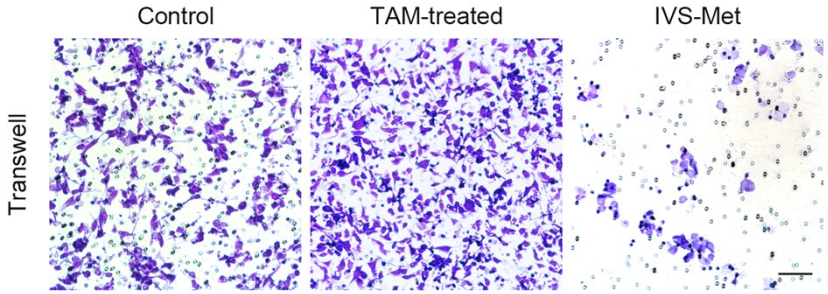

Figure S20. The invasive ability of tumor cells after various treatment. The transwell assay of B16F10 cells in control (without treatment), TAM-treated (co-incubated with TAMs), and IVS-Met (treated with TAMs and IVS-Met) group at 48 h. Scale bar: 50 μm. Tumor cells exhibited enhanced invasive ability when co-incubated with TAMs. However, the invasion of tumor cells was significantly inhibited after treatment with IVS-Met.

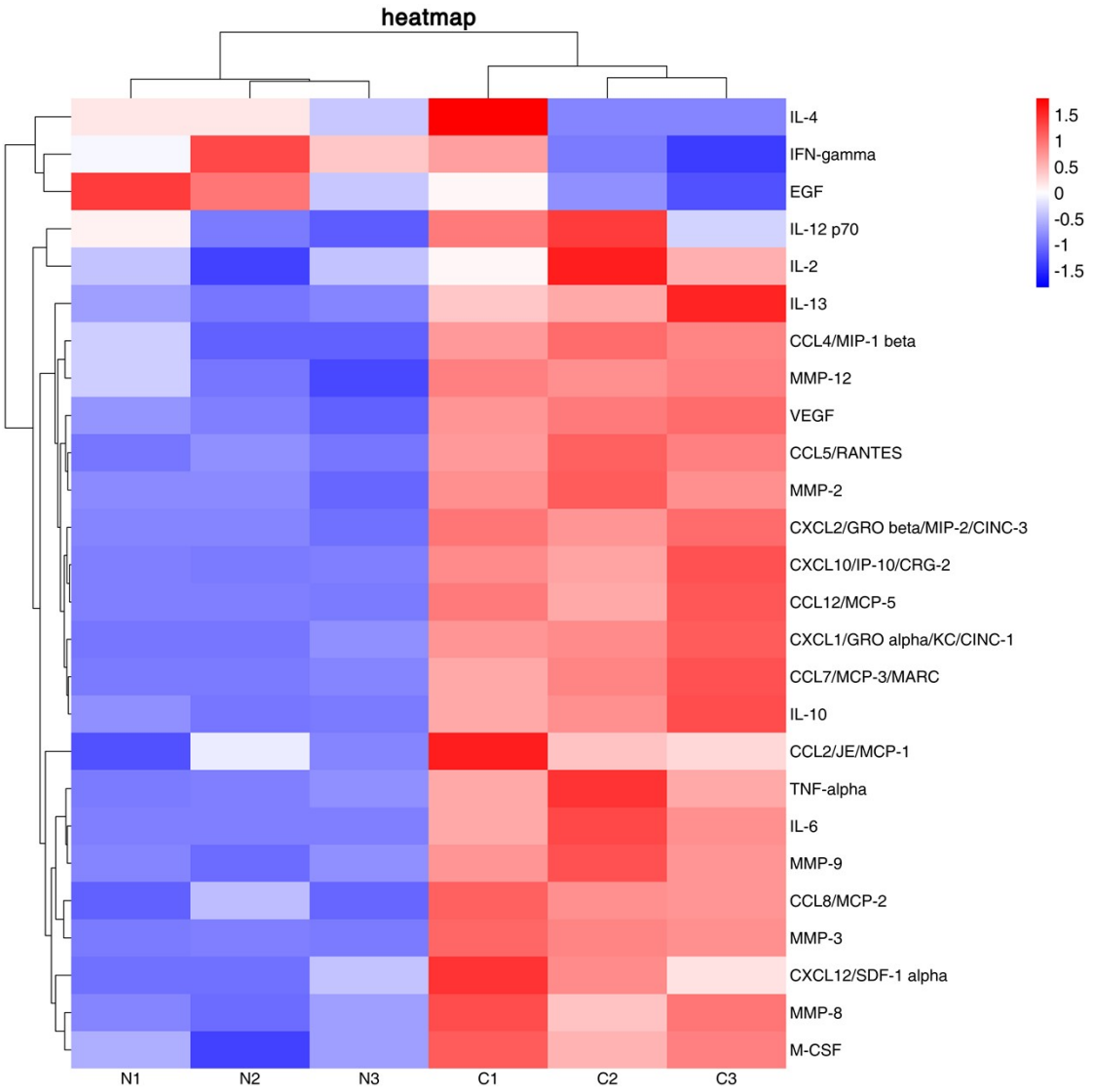

Figure S21. Heatmap of the expression of inflammation-associated cytokines. Differentially expressed cytokines between BMMs (N1-N3) and BMMs+Tu (C1-C3) group. Red corresponds to up-regulation; blue to down-expression. The expression of CCL2, CCL5, MMP8, MMP9, and MMP12 of BMMs after co-incubation with tumor cells increased compared with BMMs alone.

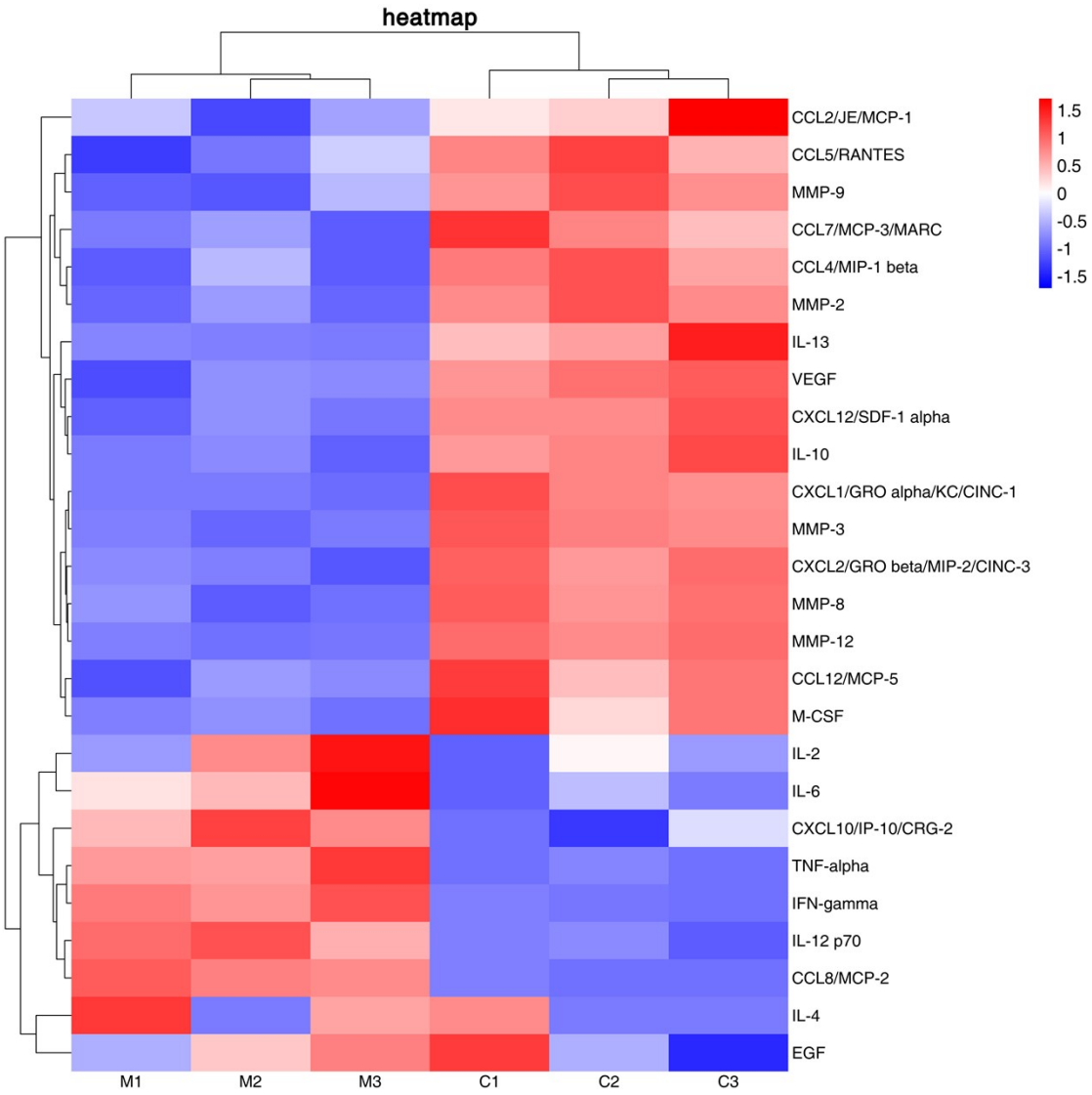

Figure S22. Heatmap of the expression of inflammation-associated cytokines. Differentially expressed cytokines between BMMs+Tu (C1-C3) and BMMs+Tu+IVS-Met (M1-M3) group. Red corresponds to up-regulation; blue to down-expression. The expression of CCL2, CCL5, MMP8, MMP9, and MMP12 decreased after IVS-Met treatment.

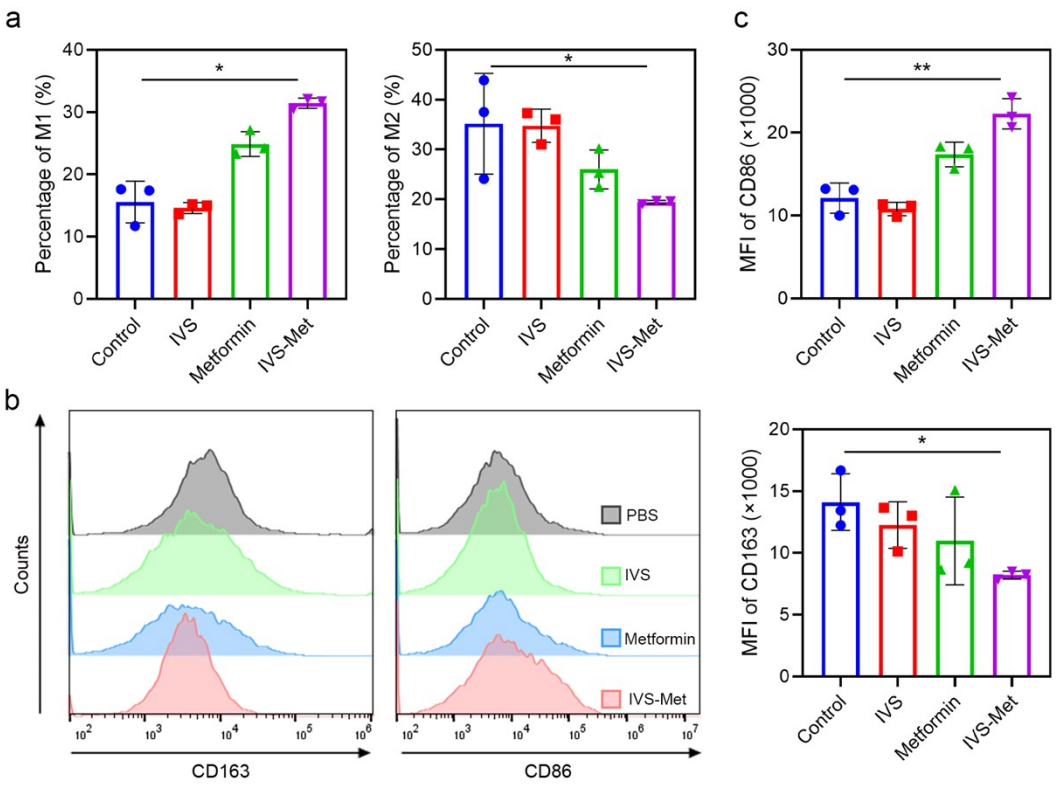

Figure S23. TAM polarization effect of IVS-Met *in vivo*. a) Quantitative analysis of the amount of M1 and M2 TAMs from flow cytometry results (n = 3). b) Representative histograms of the expression of cell surface marker CD163 and CD86 in each group. After treated with IVS-Met, the expression of CD163 reduced. c) Quantitative analysis of CD163 and CD86 (MFI) from flow cytometry (n = 3). The statistical significance was measured by Student's *t*-test (* $P < 0.05$, ** $P < 0.01$). These results revealed that IVS-Met could reduce the proportion of M2 TAMs and induce M1 TAMs in TME.

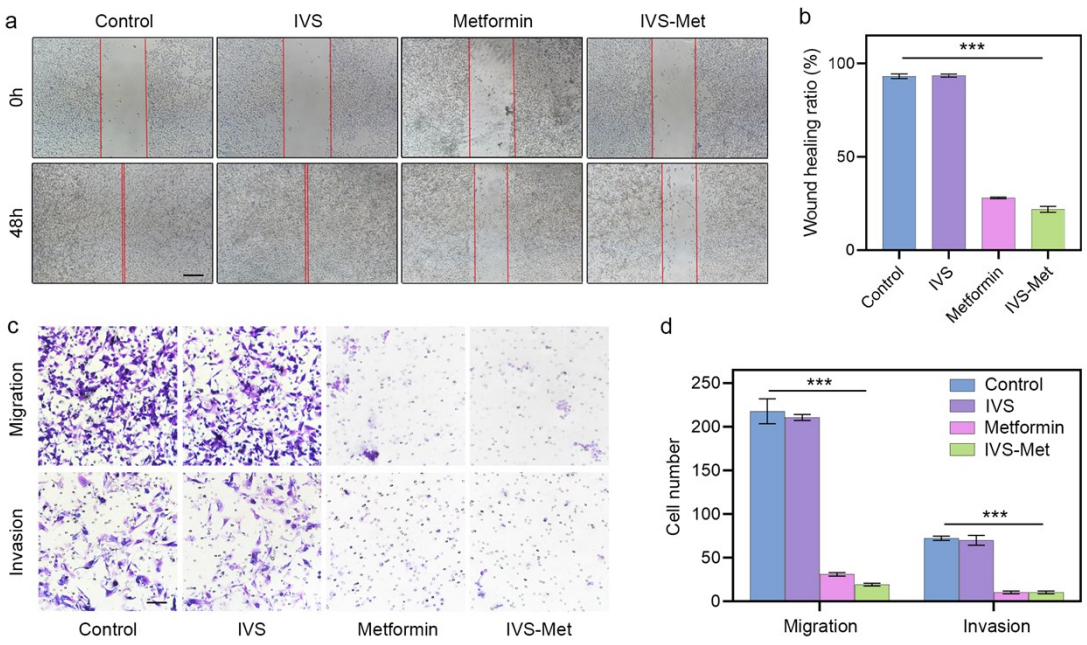

Figure S24. The *in vitro* evaluation of the migration and invasion ability of tumor cells. a) Wound-healing assay in each group. Scale bar: 100 μm. b) Quantitative analysis of the wound healing ratio. c) Transwell migration and invasion assays. Scale bar: 50 μm. d) Quantitative analysis of the migration and invasion ratio in each group. The statistical significance was measured by Student's *t*-test (*** $P < 0.001$). The inhibition rates of IVS-Met on the migration and invasion of tumor cells were 91.1% and 85.7%, respectively.

2. Supplementary tables

Table S1. Sequences of primers utilized in this paper

Name	Primer sequence (5'-3')
Tnf-F	TAGCCCACGTCGTAGCAAAC
Tnf-R	GCAGCCTTGTCCCTTGAAGA
Nos2-F	GGTGAAGGGACTGAGCTGTT
Nos2-R	ACGTTCTCCGTTCTCTTGCAG
Arg1-F	TTCTCAAAAGGACAGCCTCG
Arg1-R	CAGACCGTGGGTTCTTCACA
Mrc1-F	TTCAGCTATTGGACGCGAGG
Mrc1-R	GAATCTGACACCCAGCGGAA
Il6-F	CTCATTCTGCTCTGGAGCCC
Il6-R	CAACTGGATGGAAGTCTCTTGC
Il10-F	GTAGAAGTGATGCCCCAGGC
Il10-R	CACCTTGGTCTTGGAGCTTATT
Gapdh-F	GATAAGCAGGGCGGGAGG
Gapdh-R	CCCAATACGGCCAAATCCGT

Table S2. Killing rate of tumor cells in each group

Treatment	Killing rate (%)		
	24 h	48 h	72 h
IVS	13.73	2.02	1.31
Metformin	30.35	48.99	12.01
IVS-Met	32.23	70.46	72.83

Table S3. Percentages of M1 and M2 TAMs in each group

Group	Percentage of M1 (%)	Percentage of M2 (%)	M1/M2

Control	15.56667	35.16667	0.442654
IVS	14.6	34.76667	0.419942
Metformin	24.86667	26	0.95641
IVS-Met	31.43333	19.43333	1.617496

Table S4. The median survival time in each group

Group	Median survival time (d)
Control	20
IVS	22
Metformin	27
IVS-Met	>43